Physics – Uspekhi **59** (2) 168 – 173 (2016)

CONFERENCES AND SYMPOSIA

PACS numbers: 32.30.Jc, 37.10.De, 37.10.Gh

Ultracold lanthanides: from optical clock to a quantum simulator

G A Vishnyakova, A A Golovizin, E S Kalganova, V N Sorokin,
D D Sukachev, D O Tregubov, K Yu Khabarova, N N Kolachevsky

DOI: 10.3367/UFNe.0186.201602h.0176

Contents

1. **Introduction** 168
2. **Deep laser cooling of thulium atoms** 169
3. **Observation of the 1.14 μm magnetic dipole transition** 170
4. **Ultrastable laser systems** 171
5. **Quantum simulations** 172
6. **Conclusions** 172
References 173

Abstract. We review the current research on precision spectroscopy and quantum optics applications of laser-cooled lanthanides. We discuss the specific electronic structure of hollow atoms, which determine prospects for application in optical frequency standards and in quantum simulators based on spin interactions in optical lattices. Using the example of the thulium atom, we describe the specifics of laser cooling, optical lattice trapping techniques, and clock transition spectroscopy using spectrally narrow lasers.

Keywords: laser cooling, lanthanides, optical frequency standards, ultrastable laser systems, quantum simulations

1. Introduction

The field of laser cooling of rare-earth elements was being rapidly developed in the last decade. The closed outer $6s^2$ shell of these elements makes them similar to alkaline-earth elements; however, the spectra of rare-earth atoms prove to be considerably more complicated due to the inner f and d shells. Progress in the development of laser cooling of this group of atoms seems to have been restrained for a long time just by this factor: at first glance, neither of the rare-earth atoms has the strong closed transitions required for efficient laser cooling. A decisive breakthrough was achieved by a group in the USA in 2006, which demonstrated the laser cooling of erbium atoms at a wavelength of 400.1 nm [1]. All the numerous possible decay channels of the upper cooling level proved to be too weak to considerably affect the laser cooling process. The laser cooling of dysprosium [2], thulium, and holmium [3] was demonstrated somewhat later. The laser cooling of thulium atoms was first demonstrated by our group at the Lebedev Physical Institute, RAS (FIAN) in 2010 [4]. At present, studies of ultracold lanthanides are being performed in the USA, Russia, Germany, and Austria, where the interactions of strongly magnetic atoms are investigated at ultralow temperatures and new frequency standards are being developed.

Most lanthanides have an incomplete inner 4f shell and large ground-state fine splitting. In addition, such transitions are forbidden in the electric dipole approximation, and therefore have a small spectral width. Earlier, we performed a series of studies on coherent population trapping in samarium vapors at transitions in the ground-state fine structure [5]. The combination of the high transition frequency (up to an optical frequency) with long coherence times (about 1 s) makes lanthanides promising candidates for use in modern optical clocks [6].

A parallel avenue in the use of ultracold lanthanides is the study of their interactions at ultralow temperatures. A specific feature of lanthanides with incomplete inner electron shells is the large ground-state magnetic dipole moment, which can reach 12 Bohr magnetons. Because of the long-range character of dipole–dipole interaction and its anisotropy, a number of quantum effects taking place in solids can be reproduced in atomic ensembles. Despite the difference in scales (a few hundred nanometers in atomic ensembles and a few fractions of a nanometer in solids), the interaction Hamiltonians turn out to be identical, which allows predicting a number of properties of a solid with the help of such atomic 'simulators'. It was found that the strength of the interaction between atoms and its sign, i.e., whether the

G A Vishnyakova, A A Golovizin, E S Kalganova, D O Tregubov, K Yu Khabarova Lebedev Physical Institute,
Russian Academy of Sciences,
Leninskii prosp. 53, 119991 Moscow, Russian Federation;
Moscow Institute of Physics and Technology (State University),
Institutskii per. 9, 141700 Dolgoprudnyi, Moscow region,
Russian Federation
E-mail: gulnarav7@gmail.com, artem.golovizin@gmail.com,
kalganova.elena@gmail.com, treg.dim@gmail.com,
kseniakhabarova@gmail.com
V N Sorokin, D D Sukachev, N N Kolachevsky Lebedev Physical Institute,
Russian Academy of Sciences,
Leninskii prosp. 53, 119991 Moscow, Russian Federation
E-mail: sovn@sci.lebedev.ru, sukachev@gmail.com,
kolachevsky@lebedev.ru

Received 30 November 2015
Uspekhi Fizicheskikh Nauk **186** (2) 176 – 182 (2016)
DOI: 10.3367/UFNr.0186.201602h.0176
Translated by M Sapozhnikov; edited by A M Semikhatov

interaction is attractive or repulsive, can be controlled, for example, with the help of Feshbach resonances in an external magnetic field [7]. This opens up a unique possibility to study magnetic properties, phase transitions, and other processes by changing the interaction Hamiltonian using the same atomic ensemble.

In this paper, we consider some applications of ultracold lanthanides using the example of laser-cooled thulium atoms. In Section 2, we present our recent results on second-stage cooling at a wavelength of 530.7 nm. Section 3 is devoted to the study of a 1.14 μm magnetic dipole transition that we plan to use to create stable and precise optical clocks. In Section 4, we describe the current state and consider the prospects for the development of ultrastable laser systems in our group for laser cooling and clock transition spectroscopy. In Section 5, a brief review of possible applications of lanthanides to address the challenge of quantum simulators is presented.

2. Deep laser cooling of thulium atoms

At the first stage of laser cooling and trapping of thulium atoms in a magneto-optical trap (MOT), we used the 410.6 nm transition with the natural width $\gamma_1 = 10$ MHz (Fig. 1). This corresponds to the Doppler temperature limit of 240 μK. However, because of the close values of Landé g-factors of cooling levels, the sub-Doppler cooling mechanism [8] works efficiently directly in the MOT. Due to such a specific feature, a temperature of 25 μK was achieved without using special techniques. Details of experiments on first-stage laser cooling and trapping of thulium atoms are described in [4, 6].

For a deeper cooling, we used the narrow 530.7 nm transition with the natural width $\gamma_2 = 350$ kHz, corresponding to the Doppler limit of 9 μK. The second harmonic of a Toptica DL-pro semiconductor laser was used as a cooling light source. The laser radiation frequency was stabilized with a high-Q stable ULE (Ultra Low Expansion) glass resonator. The stabilization method and laser parameters are presented in Section 4. Stabilization is required to narrow the laser linewidth, which should be much narrower than the natural width γ_2 of the cooling transition. In addition, stabilization makes tuning to the transition frequency considerably easier due to the high long-term stability of the laser frequency.

We used a classical MOT scheme [10] in experiments. Three pairs of mutually orthogonal beams (two couterpropagating beams with circular polarizations with opposite signs in each pair) created a three-dimensional optical molasses at the center of a vacuum chamber. A quadrupole magnetic field was produced with the help of a pair of coils in the anti-Helmholtz configuration. Circularly polarized 410.6 nm radiation was used for Zeeman slowing [11]. The first-stage and second-stage cooling beams were combined on polarization beamsplitters, and the atoms were loaded into the MOT for 1 s. Then, first-stage cooling beams were switched off and the atoms were additionally cooled in the second-stage MOT for 30–50 ms. The second-stage cooling experiment is described in detail in [12].

The temperature of the atoms was measured by the ballistic expansion method. For this purpose, the cooling radiation and magnetic field were switched off after the MOT loading, and then the cloud was illuminated after a time t (0–10 ms) by a resonance 410.6 nm pulse and a photograph of the luminescing cloud was recorded.

Figure 2 presents the shape of the atomic cloud before its expansion and its temperature depending on the second-stage cooling laser detuning. The light intensity in this series of measurements was 75 μW per beam, corresponding to the saturation parameter $S = 2$ at the trap center. The minimum temperature was 8 μK along the horizontal axis and 16 μK along the vertical axis. It can be seen from Fig. 2 that as the detuning increases, the cloud moves downwards and the temperature becomes independent of detuning. This is explained by the fact that gravity plays a noticeable role during cooling at a narrow transition. At large detunings of cooling radiation, the trap depth decreases and gravitation causes a displacement of the potential minimum downwards [13]. The cloud falls within a nonzero magnetic field region and the appearing Zeeman shift of atomic levels begins to compensate the frequency detuning of cooling radiation, with the effective detuning remaining constant and temperature being invariable.

The use of a narrow transition for laser cooling also allows observing other interesting effects, for example, the formation of momentum-space crystals. This phenomenon, appearing during the change of the negative sign of the cooling radiation frequency to the positive sign, consists in the

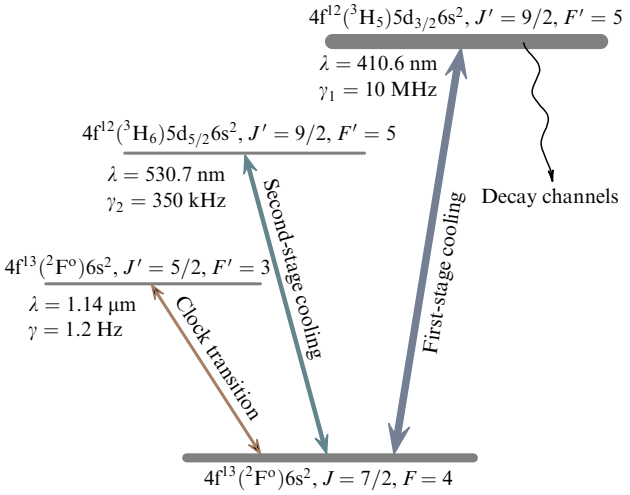

Figure 1. Energy level diagram of thulium atoms involved in experiments.

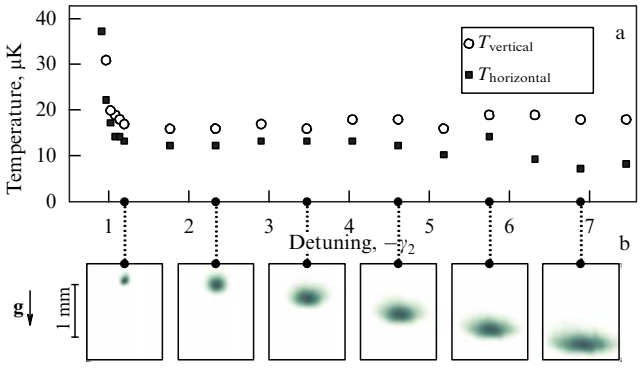

Figure 2. (a) Dependence of the atomic cloud temperature in a MOT on the laser detuning in the second-stage cooling cycle. Circles corresponds to the ensemble temperature in the vertical direction and squares, to temperature in the horizontal direction. The cloud temperature was measured by the ballistic expansion technique. (b) Shape and position of the cloud in the MOT before expansion corresponding to the indicated frequency detuning.

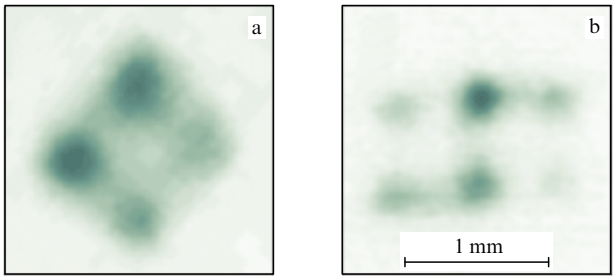

Figure 3. Formation of a momentum-space crystal. A cloud of Tm atoms separates into eight groups flying apart along the principal diagonals of a cube. (a) Top and (b) side views of the atomic cloud after a 2 ms expansion.

separation of atoms into several velocity groups whose position in the momentum space resembles a cubic crystal lattice. Such a behavior of an ensemble is explained by the fact that for a positive detuning of cooling radiation, the MOT light does not decelerate atoms but accelerates them along the direction of the beams. As the atoms are accelerated, the frequency detuning in the reference frame connected with an atom increases due to the Doppler effect, and the atom interacts with light more weakly. As a result, this process is stabilized at some equilibrium velocity [13].

The separation of the atomic ensemble into subgroups in the momentum space is revealed in the coordinate space in the picture of the expansion of an atomic cloud, which separates into eight parts located in the vertices of a cube. To obtain such crystals in the momentum space, the atoms were captured in the second-stage MOT, as described above. The sign of the cooling radiation detuning was then changed, and the atomic cloud began to expand in a characteristic way (Fig. 3).

In the nearest future, we plan to decrease the temperature by evaporation cooling in an optical dipole trap and to study the distribution of atoms over the magnetic sublevels after the second-stage cooling.

3. Observation of the 1.14 μm magnetic dipole transition

A specific feature of the thulium atom is the presence of the ground-state fine structure with a 263 THz transition frequency (see Fig. 1). The magnetic dipole transition coupling these two levels has a natural linewidth of about 1 Hz and the wavelength 1.14 μm, which makes it a promising candidate for use as an optical frequency reference [6]. Theoretical calculations of the excitation probability for this transition under real experimental conditions and the first experimental observation of the resonance excitation of the transition in a cloud of cold thulium atoms are presented in [14].

To develop optical clocks, it is necessary to capture atoms in an optical dipole trap providing: (i) the absence of resonance radiation; (ii) the absence of a magnetic field; (iii) the confinement of atoms in both the ground and excited states of the clock transition; and (iv) the removal of Doppler broadening (the Lamb–Dicke regime in an optical lattice [15]). An optical dipole trap was created using an 8 W single-frequency Coherent Verdi-V8 laser emitting at 532 nm. The use of a retroreflector allows creating a one-dimensional optical lattice, i.e., a dipole trap in the form of a standing wave. The first results of the recapture of atoms from a MOT after the first-stage cooling to a dipole trap showed an efficiency of $\sim 1\%$, which was caused by the high temperature (100 μK) of atoms after the first-stage cooling. Another factor reducing the recapturing efficiency was the large size of the MOT cloud, equal to 200 μm for a dipole trap waist equal to 50 μm. Second-stage cooling described above considerably reduced the cloud temperature. The use of second-stage cooling resulted in an increase in the efficiency of recapturing from the MOT to the optical lattice to 50%.

We recorded the excitation profile of the 1.14 μm magnetic dipole transition in thulium atoms captured in an optical trap. After the first-stage and second-stage cooling, the atoms are captured in the optical lattice, with $(1-5)\times 10^5$ atoms accumulated in the $50\times 50\times 100$ μm region at a temperature of 10–20 μK. Then, 1.14 μm clock laser radiation is switched on for 1 ms to excite the magnetic dipole transition. The laser output power is 360 μW, which corresponds to the saturation parameter 3×10^9. The laser frequency is stabilized with a high-Q ULE resonator (see Section 4), which narrows the laser linewidth to less than 100 Hz.

The 1.14 μm resonance radiation excites some of the atoms to the upper sublevel of the clock transition (see Fig. 1). The number of atoms remaining in the ground state is measured by the resonance luminescence signal at 410.6 nm.

Figure 4 shows the spectral profiles of the magnetic dipole transition for two excitation regimes: (i) in the optical dipole trap (circles) and (ii) after switching the dipole trap off (triangles). The spectral width of the magnetic dipole transition profile recorded in the first case was 1 MHz. This width contains contributions from the Doppler broadening (0.05 MHz), Zeeman splitting in a residual magnetic field (0.4 MHz), broadening caused by tensor polarizability at the trap wavelength of 532 nm and inhomogeneity of the optical lattice potential (0.4 MHz), and power broadening by excitation light (< 0.1 MHz).

If the atoms are released from the optical dipole trap, the spectral width of the clock transition line decreases to 0.6 MHz, which is explained by elimination of the trap potential contribution. Figure 4 shows that the transition frequency also changes because of different dynamic polariz-

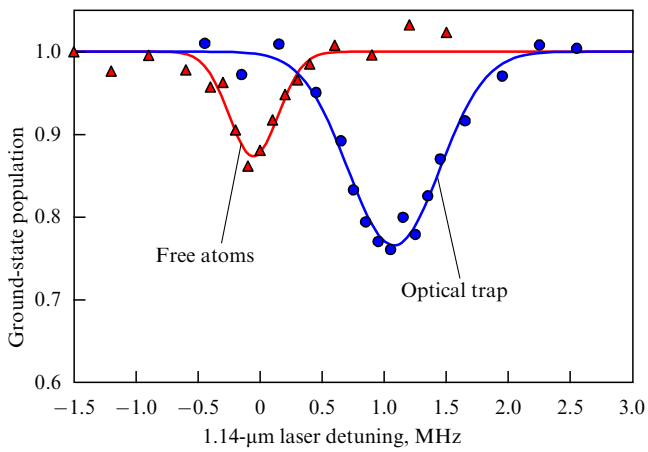

Figure 4. Ground-state population as a function of the 1.14 μm radiation detuning. Circles are measurements in the optical trap, triangles are measurements after the release of atoms from the MOT. Solid curves are the approximations of experimental points by a Gaussian. The profile width is 1 MHz for the switched-on optical lattice and 0.6 MHz for the switched-off lattice.

abilities of the lower and upper levels at a wavelength of 532 nm.

Our experimental results show that in order to develop optical clocks, it is necessary to load atoms into an optical lattice produced at the 'magic' wavelength at which the dynamic polarizabilities of the upper and lower levels of the clock transition become identical [16]. We plan to search for the magic wavelength using radiation from a Ti:Sa laser in the wavelength range from 700 to 800 nm.

4. Ultrastable laser systems

In the last decade, considerable progress has been observed in the development of optical atomic clocks. With the advent of a new era in optical frequency measurements [17], their stability has increased by two orders of magnitude over that of cesium fountains, which are the best primary frequency standards. To excite narrow optical transitions, the linewidth of the exciting ('clock') laser should be minimal. The laser system itself must have high frequency stability at time intervals up to 10 s to ensure the accumulation of data read from atoms. To solve these problems, the laser is typically actively stabilized by an external high-Q Fabry–Perot resonator. The stabilization setup is described in detail in [18].

Today, high stability parameters are provided by ULE glass resonators [19]. ULE glass is optically transparent in a broad wavelength range and has a zero linear coefficient of thermal expansion at temperatures close to room temperature [18]. Our group at FIAN manufactured and tested a number of laser systems stabilized by high-Q ULE glass resonators. These systems are used for secondary cooling of thulium (530.7 nm) (see Section 2) and strontium (689 nm) atoms [18] and for recording the clock transition in thulium (1140 nm) and strontium (698 nm) atoms.

Figure 5 presents the normalized Allan deviation obtained by comparing two identical laser systems at a wavelength of 698 nm, developed at FIAN. With the linear drift ignored, the mutual instability of the two systems for averaging times up to 100 s remains at a level of 3×10^{-15}, approaching the limit of thermal noise produced by resonators, substrates, and mirror coatings. All other laser systems mentioned above are expected to have similar characteristics.

Thermal noise arises due to random relative motion of the surface of cavity mirrors caused by thermally excited vibrational modes of the cavity spacer, mirror substrates, and the multilayer mirror coating. Fluctuations of mirror surfaces change the resonator length and frequency fluctuations. The spectral density of thermal noise introduced by the cavity spacer is described by the expression [20]

$$S_{\text{spacer}}(\omega) = \frac{4k_{\text{B}}T}{\omega}\,\frac{L}{3\pi R^2 E}\,\phi_{\text{spacer}}\,, \qquad (1)$$

where T is the cavity body temperature, k_{B} is the Boltzmann constant, L is the resonator length, R is the radius of the cavity spacer, E is Young's modulus of the material, and ϕ_{spacer} is the mechanical loss coefficient.

Young's modulus of ULE glass is $E = 6.8 \times 10^{10}$ Pa. The loss coefficient is inversely proportional to the Q factor: $\phi_{\text{spacer}} = Q^{-1}_{\text{spacer}} = 1.7 \times 10^{-5}$.

Thermal noises introduced by mirror substrates are described by the expression

$$S_{\text{mirror}}(\omega) = \frac{4k_{\text{B}}T}{\omega}\,\frac{1-\sigma^2}{\sqrt{\pi}Ew_0}\,\phi_{\text{sub}}\,, \qquad (2)$$

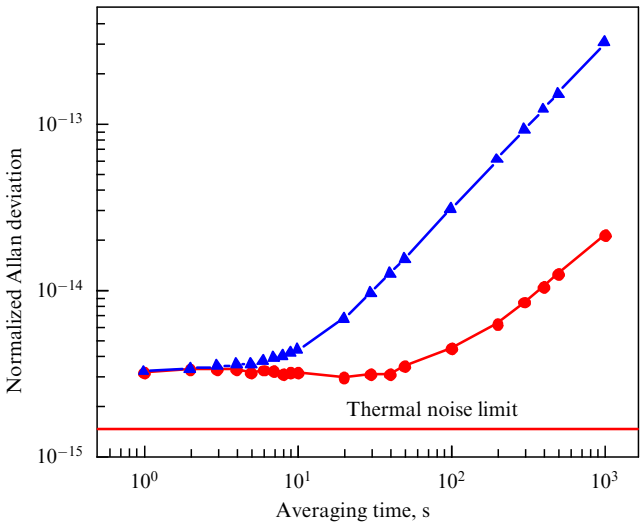

Figure 5. Normalized Allan deviation obtained by comparing two identical laser systems at a wavelength of 698 nm independently stabilized by ultrastable Fabry–Perot resonators (triangles). The recrystallization of ULE glass causes a linear frequency drift ~ 180 mHz s^{-1}. Circles show the same after the linear drift compensation.

where $\sigma = 0.18$ is the Poisson ratio for ULE glass, and w_0 is the waist radius on the mirror (usually 200–500 μm). Mirror substrates are also made of ULE glass, and therefore $\phi_{\text{spacer}} = \phi_{\text{sub}}$.

Thermal noises introduced by the multilayer coating of mirrors are additionally determined by the multilayer coating thickness and the high loss coefficient,

$$S_{\text{coat}}(\omega) = S_{\text{mirror}}\left(1 + \frac{2}{\sqrt{\pi}}\,\frac{1-2\sigma}{1-\sigma}\,\frac{\phi_{\text{coat}}}{\phi_{\text{sub}}}\,\frac{d}{w_0}\right), \qquad (3)$$

where $\phi_{\text{coat}} = 25\,\phi_{\text{spacer}}$ is the loss coefficient in the deposited material (as a rule, SiO_2 and Ta_2O_5 layers). The multilayer structure thickness is $d \approx 2$ μm. Thermal noises impose a fundamental restriction on the frequency stability achieved using such a material. Obviously, the thermal noise limit can be reduced by lowering the temperature and choosing materials with better mechanical parameters.

One promising material is monocrystalline silicon [21]. This material is optically transparent at wavelengths above 1.2 μm, has a low loss coefficient $\phi < 10^{-7}$, and has Young's modulus three times higher than that of quartz. In addition, monocrystalline silicon has a crystal temperature close to 124 K (at this point, the linear coefficient of thermal expansion vanishes), and recrystallization processes inherent in ULE are absent in it. In [21], the stability of laser systems based on monocrystalline silicon cavities was demonstrated at a level of 2×10^{-16} for 1 s. In this case, multilayer mirror coatings made the main contribution to thermal noise in the systems.

Thermal noise can be reduced further by passing from dielectric reflecting coatings to crystalline coatings, which provides an increase in Young's modulus and the mechanical Q factor of the coating material, resulting in a further reduction in the thermal noise limit (3). It was shown in [22] that the use of a mirror with a semiconductor crystalline reflecting coating (AlGaAs/GaAs) provides an order-of-magnitude decrease in the thermal noise level introduced by mirror coatings. Such coatings have excellent optical proper-

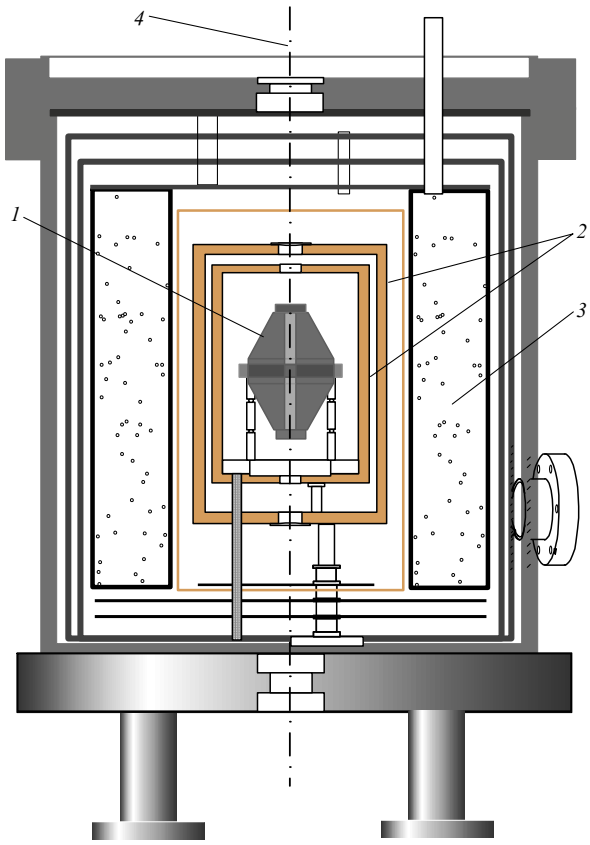

Figure 6. Vacuum chamber of a monocrystalline silicon resonator: (*1*) resonator body; (*2*) thermal shields; (*3*) cold nitrogen reservoir; (4) optical axis.

ties at wavelengths above 1 μm, providing cavity finesse above 10^5.

Our group at FIAN, in collaboration with researchers at the All-Russian Research Institute of Physicotechnical and Radio Engineering Measurements (VNIIFTRI), began work on the development of a laser system stabilized by a high-Q monocrystalline silicon Fabry–Perot resonator with mirrors with crystalline reflecting coatings. The resonator will be cooled to 124 K with a cold nitrogen flow (Fig. 6). The gas flow is supplied through a bellows into a toroidal reservoir around the cavity. The cavity is surrounded with heat-insulating jackets to minimize its temperature variations. We expect that the frequency instability of the laser system stabilized with respect to this cavity will be reduced to 10^{-17}.

5. Quantum simulations

Technological progress in recent decades is closely related to the synthesis of new materials used in various fields of science and technology. As Vitalii Ginzburg predicted, the creation of a room-temperature superconductor will be of great importance [23–27]. And, although virtually any compound can presently be synthesized in chemical laboratories, the search for materials having the required set of properties remains an unsolved quantum mechanical problem because of the enormous computational complexity [28].

Ultracold atoms confined in an optical trap [29] are the ideal model of a particle (electron) moving in the periodic potential of an atomic lattice [30]. It has been proposed to use such systems for simulating processes taking place in solids [31, 32]. This requires an approximate coincidence of the Hamiltonian of atoms in the optical lattice with the electronic Hamiltonian in a solid [33]. The required Hamiltonian can be 'synthesized', for example, using a train of laser pulses producing effective gauge fields [34, 35], or with the help of Feshbach resonances [7], which change the scattering length of atoms in a broad range, or by varying the optical potential itself. Simultaneously, using the atoms of two different elements [36] (or identical atoms in different quantum states), it is possible to imitate the electron spin, while changing the optical potential locally allows taking defects in a solid into account. Because characteristic evolution times are about 1 ms, the real-time control of the system dynamics is possible. Moreover, because the individual sites of the lattice can be optically resolved [37, 38], it is possible not only to measure the 'macroscopic' properties of the system but also to study quantum entanglement [39]. The possibility of studying one-dimensional, two-dimensional, and three-dimensional systems has emerged.

Today, proof-of-principle experiments are being performed that confirm the possibility of simulations of the properties of solids by using atomic gases [40–42]. A number of effects such as magnetism [43], Bloch oscillations [44], and the metal–dielectric transition [45, 46] have been reproduced.

In most of the papers mentioned above, the interaction between atoms was short-range, i.e., it was sufficient to take the interaction only between neighboring atoms into account. The use of rare-earth atoms with a large ground-state magnetic moment adds the potential of magnetic dipole interaction and considerably extends simulation possibilities [47, 48]. The thulium atom stands out among other rare-earth atoms by its relatively simple energy level diagram [49], which simplifies the control of the internal states of the atom. In addition, in other experiments, an optical lattice is created using near-IR laser radiation, whereas thulium can be trapped in lattices at a wavelength of 532 nm [50], which enhances the magnetic dipole–dipole interaction by almost an order of magnitude.

Feshbach resonances allow changing the scattering length of atoms by varying an external magnetic field. These resonances most often fall in the range from a few hundred to a few thousand gauss [7], which poses technical difficulties related to the production and stabilization of the magnetic field. Recent measurements of rare-earth Er [51] and Dy [52] atoms have shown the presence of many Feshbach resonances in the region of magnetic fields on the order of a few gauss, which greatly simplifies the configuration of experiments. This specific feature of rare-earth atoms is explained by their anisotropic interaction with each other [53]. We can expect that thulium also has a number of strong Feshbach resonances in weak magnetic fields. These resonances are being studied at our laboratory at FIAN.

6. Conclusions

Some specific properties of laser-cooled lanthanides have been demonstrated using the example of the rare-earth thulium atom. The formation of momentum-space crystals has been demonstrated by irradiation of a cold atomic cloud by a narrow-line laser with blue frequency detuning. The 1.14 μm magnetic dipole transition between the ground-state fine structure components were studied.

It has been shown that the spectral broadening of the transition is manly determined by the inhomogeneous broad-

ening in the gradient of the light field of the optical dipole trap caused by different dynamic polarizabilities of the levels and also by the large tensor polarizability.

We plan to proceed to the magic wavelength, which should eliminate light shifts and open the possibility of approaching the realization of thulium optical clocks.

Progress is presented on the development of ultrastable laser systems using ULE resonators and in a new direction, the development of cryogenic resonators based on crystalline structures. This approach should suppress thermal noise by two orders of magnitude and provide relative instability of laser systems at a level of 10^{-17} per second.

Possible applications of thulium atoms and other rare-earth elements to the challenge of quantum simulators have been described, which can bring the creation of room-temperature superconductors closer.

Acknowledgements
The work was supported by the Russian Foundation for Basic Research (grants 15-02-03936 and 15-02-05324).

References

1. McClelland J J, Hanssen J L *Phys. Rev. Lett.* **96** 143005 (2006)
2. Youn S H et al. *Phys. Rev. A* **82** 043425 (2010)
3. Miao J et al. *Phys. Rev. A* **89** 041401 (2014)
4. Sukachev D et al. *Phys. Rev. A* **82** 011405(R) (2010)
5. Kolachevskii N N et al. *Quantum Electron.* **31** 61 (2001); *Kvantovaya Elektron.* **31** 61 (2001)
6. Kolachevsky N N *Phys. Usp.* **54** 863 (2011); *Usp. Fiz. Nauk* **181** 896 (2011)
7. Chin C et al. *Rev. Mod. Phys.* **82** 1225 (2010)
8. Dalibard J, Cohen-Tannoudji C *J. Opt. Soc. Am. B* **6** 2023 (1989)
9. Sukachev D D et al. *JETP Lett.* **92** 703 (2010); *Pis'ma Zh. Eksp. Teor. Fiz.* **92** 772 (2010)
10. Raab E L et al. *Phys. Rev. Lett.* **59** 2631 (1987)
11. Chebakov K et al. *Opt. Lett.* **34** 2955 (2009)
12. Vishnyakova G A et al. *Laser Phys.* **24** 074018 (2014)
13. Loftus T H et al. *Phys. Rev. A* **70** 063413 (2004)
14. Golovizin A A et al. *Quantum Electron.* **45** 482 (2015); *Kvantovaya Elektron.* **45** 482 (2015)
15. Eschner J et al. *J. Opt. Soc. Am. B* **20** 1003 (2003)
16. Hidetoshi K *Nature Photon.* **5** 203 (2011)
17. Udem Th, Holzwarth R, Hänsch T W *Nature* **416** 233 (2002)
18. Khabarova K Yu et al. *Quantum Electron.* **42** 1021 (2012); *Kvantovaya Elektron.* **42** 1021 (2012)
19. Corning Incorporated, Corning Code 7972 Ultra Low Expansion Glass, http://www.corning.com/media/worldwide/csm/documents/D20FD2EA-7264-43DD-B544-E1CA042B486A.pdf
20. Numata K, Kemery A, Camp J *Phys. Rev. Lett.* **93** 250602 (2004)
21. Kessler T et al. *Nature Photon.* **6** 687 (2012)
22. Cole G et al. *Nature Photon.* **7** 644 (2013)
23. Ginzburg V L, Kirzhnits D A *Sov. Phys. Usp.* **30** 671 (1987); *Usp. Fiz. Nauk* **152** 575 (1987)
24. Ginzburg V L *Phys. Usp.* **48** 173 (2005); *Usp. Fiz. Nauk* **175** 187 (2005)
25. Schrieffer J R *Handbook of High-Temperature Superconductivity. Theory and Experiment* (New York: Springer, 2007)
26. Putilin S N et al. *Nature* **362** 226 (1993)
27. Bednorz J G, Müller K A *Z. Phys. B* **64** 189 (1986)
28. Troyer M, Wiese U-J *Phys. Rev. Lett.* **94** 170201 (2005)
29. Bloch I *Nature Phys.* **1** 23 (2005)
30. Köhl M et al. *Phys. Rev. Lett.* **94** 080403 (2005)
31. Bloch I et al. *Nature Phys.* **8** 267 (2012)
32. Lewenstein M et al. *Adv. Phys.* **56** 243 (2007)
33. Feynman R P *Int. J. Theor. Phys.* **21** 467 (1982)
34. Dalibard J et al. *Rev. Mod. Phys.* **83** 1523 (2011)
35. Aidelsburger M et al. *Phys. Rev. Lett.* **107** 255301 (2011)
36. Mosk A et al. *Appl. Phys. B* **73** 791 (2001)
37. Bakr W S et al. *Nature* **462** 74 (2009)
38. Parsons M F et al. *Phys. Rev. Lett.* **114** 213002 (2015)
39. Islam R et al., arXiv:1509.01160
40. Schneider U et al. *Science* **322** 1520 (2008)
41. Chin J K et al. *Nature* **443** 961 (2006)
42. Martiyanov K et al. *Phys. Rev. Lett.* **105** 030404 (2010)
43. Simon J et al. *Nature* **472** 307 (2011)
44. Mandel O et al. *Phys. Rev. Lett.* **91** 010407 (2003)
45. Greiner M et al. *Nature* **415** 39 (2002)
46. Jördens R et al. *Nature* **455** 204 (2008)
47. Barnett R et al. *Phys. Rev. Lett.* **96** 190401 (2006)
48. Góral K, Santos L, Lewenstein M *Phys. Rev. Lett.* **88** 170406 (2002)
49. Kolachevsky N et al. *Appl. Phys. B* **89** 589 (2007)
50. Sukachev D D et al. *Quantum Electron.* **44** 515 (2014); *Kvantovaya Elektron.* **44** 515 (2014)
51. Frisch A et al. *Nature* **507** 475 (2014)
52. Baumann K et al. *Phys. Rev. A* **89** 020701(R) (2014)
53. Petrov A,Tiesinga E, Kotochigova S *Phys. Rev. Lett.* **109** 103002 (2012)